

ENCIT-2018-0624

STUDY OF THE ASYMMETRIC TAYLOR BUBBLE RISING AGAINST A DOWNWARD FLOW

Ricardo Cavalcanti Linhares

ricklinhares@gmail.com

Igor Braga de Paula

Pontifical Catholic University of Rio de Janeiro – PUC-RJ, Rua Marquês de São Vicente, 225, Gávea, Rio de Janeiro-RJ, 22451-900, Brazil

igordepaula@puc-rio.br

Abstract. *The work is devoted to study the flow around a Taylor bubble rising against a downward flow. At this condition Taylor bubbles can exhibit an asymmetric behavior and a lower drag in comparison with symmetric ones. This flow condition is present in many industrial applications such as petrochemical, nuclear, refrigeration and many others. The characterization of the flow behavior is important for modeling the problem. However, no experiments regarding the flow around asymmetric Taylor bubble can be found in the literature due to radial oscillation of the bubble within the pipe. Therefore, averaged quantities are difficult to be measured. Here a different set-up arrangement is proposed to fix the radial position of the bubble. Thereby, Particle Image Velocimetry (PIV) measurements and image processing techniques could be applied. The experiments were carried out in a vertical pipe, using water as working fluid, at fully developed turbulent regime. Prior to velocity estimation, the images obtained had to be pre-processed in order to detect and to mask the bubble contour. Mean velocity fields around the bubble are measured for the first time and comparisons with the literature are provided.*

Keywords: *Taylor bubble, Slug flow, Multiphase flow, PIV, Counter current.*

1. INTRODUCTION

The slug flow in vertical pipes is characterized by long bubbles with a sharp shape commonly known as Taylor bubble. Dumitrescu (1943) and Davies & Taylor (1950) were one of the firsts to investigate this pattern and determine the velocity of the surrounding liquid flow. This pattern can be found in many industry processes as petroleum refining and its understanding can help to optimize these processes resulting in cost savings for companies.

The asymmetrical shape of the bubble was noticed to happen in downward flow by Griffith & Wallis (1961) and they observed that the shape of the bubble would gradually change with the increase of velocity until it get unstable.

The influence of the bubble size on its translational speed is studied by Polonsky et al. (1999). However, their studies are only for stagnant and upward flow. Nogueira et al. (2006) studied the stagnant case and the results were compatible with White and Beardmore (1962) and Polonsky et al. (1999).

This eccentricity of the bubble was justified as an attempt of the bubble to avoid the increase of velocity in the center of the tube. For this reason, when the bubble approaches the wall its speed increases.

Nicklin et al. (1962), Martin (1976) and Polonsky et al (1999) also observed the asymmetric behaviour of the bubble in downward flow and Polonsky states the difficulty concerning the oscillation of the bubble tip from one side of the pipe to another.

Most studies focuses on the behavior, shape and other parameters of the Taylor bubble, but few authors studied the flow surrounding the bubble. Goldsmith and Mason (1962) measured the velocity of the flow ahead of the bubble and in the liquid film between the wall and the bubble. through photos of the displacement of aluminum particles put on the fluid. In Kawaji et al. (1993) the photocromic dye activation method was used to measure the flow surrounding the bubble rising in stagnant fluid, obtaining instantaneous velocity ahead of the bubble. In Polonsky et al. (1999) the PIV method is used to measure the velocity surrounding the bubble, but for the liquid film it is used a tracking technique that consists in allowing the camera shutter opened. In a recent study (Nogueira et al., 2006) the shape of the bubble and the velocity profiles were determined using the PIV method and the Pulsed Shadow Technique (PST) at the same time.

However, these experiments mentioned above were only performed for stagnant and co-current flow, where the asymmetry is not likely to occur.

In (Lu and Prosperetti ,2006) an approximate analysis of stability for a rising bubble against downward flow was made and it was observed that as the flow rate increases the relative velocity between the fluid and the bubble decreases. The flattening of the bubble tip was attributed as the main reason of the instability.

Later, Jean Fabre and Bernardo Figueroa-Espinoza (2014) made further studies for different Reynolds numbers observing that not only the eccentricity of the bubble would increase with higher Reynolds but also the bubble speed. They also investigated the influence of the surface tension parameter noticing that the asymmetric bubble is much more sensitive to this parameter.

The most important factor for the bubble dynamics is the flow close to the bubble tip according to Collins et. Al (1978)

It can be seen that there is a lack of experiments regarding the characterization of the asymmetric Taylor bubble due to its variation on the radial position. This is due to radial movement of the bubble, which does not allow to estimate average quantities by using standard velocity measurement techniques such as Laser Doppler Velocimetry (LDV) and PIV. This paper presents a solution to fix the bubble position through the insertion of a small protuberance upstream of the bubble in order to create a small disturbance on the flow. This method has shown to be effective 100% of the time. Thereby, it was possible to use the PIV technique to acquire the velocity field of the surrounding flow for the first time. Results are detailed in the paper.

2. EXPERIMENTAL SET-UP

The experiments were carried out at Fluids Engineering Laboratory of Pontifical Catholic University of Rio de Janeiro. A schematic image of the experimental set-up can be seen in Fig. 1. The test bench is composed of a top reservoir (0.65 m x 0.275 m), a vertical pipe (0.026m internal diameter), a visualization box, a bottom reservoir and a centrifugal pump. The top reservoir and the pipes are made of transparent acrylic for optical access to the flow. The distance from the test section to the inlet is around 23D (0.6 m). For the flow rates investigated this is enough to ensure a developed turbulent flow at the test section. Two plates are used inside the top reservoir in order to keep a constant water column constant, hence a constant pressure at the pipe inlet. A sink was placed on the right part of the reservoir for draining the excess of water. To minimize optical distortion, a box filled with the same experiment liquid was used to encase the transparent plexiglass pipe at the test section, as suggested in the work of Nogueira et al. (2005). In order to align the flow at the entrance of the pipe it was used a honeycomb with 0.07 m height. In addition, a mesh was placed immediately downstream from the honeycomb to homogenize and reduce flow distortions.

The camera used for image acquisition was a PIV CAM 10-30 from TSI, with Nikon lens (28 mm). For PIV measurements, image acquisitions were synchronized with a pulsed red LED illuminator, model IL-105R/6X. The LED light was collimated and conditioned to form a light plane at the test section. A red optical filter was used to avoid image saturation due to the LED usage. Polystyrene particles of 50 μm were used as tracers for PIV measurements. Images were processed using standard PIV routines. Interrogation windows of 32x16 pixels and an overlap of 50% were adopted for PIV processing.

Three valves were installed to adjust the flow rate and to generate the Taylor bubble. The valves are located at approximately 18D, 18.5D and 21.5D downstream from the test section. The first valve is used to close the pipe, while the second one is a vent that allows injection of air in the pipeline. Level marks are added to the pipeline as references for controlled adjustment of the bubble volume. Flow rates are set with the third valve. The bottom reservoir is used to store the water. The electric heater and temperature sensor are placed in this tank. A PID controller is used to maintain the water temperature constant and equals to 30 °C during the tests.

In order to avoid radial oscillation of the Taylor bubble during measurements, a small protuberance was inserted in the flow. This protuberance consisted of a cylinder having a diameter of 5 mm. The cylinder intrusion was the smallest capable to fix the bubble at a constant radial position. This was achieved with a height of approximately 4 mm. The proposed methodology allowed the acquisition of mean velocity fields and use of ensemble averaging techniques.

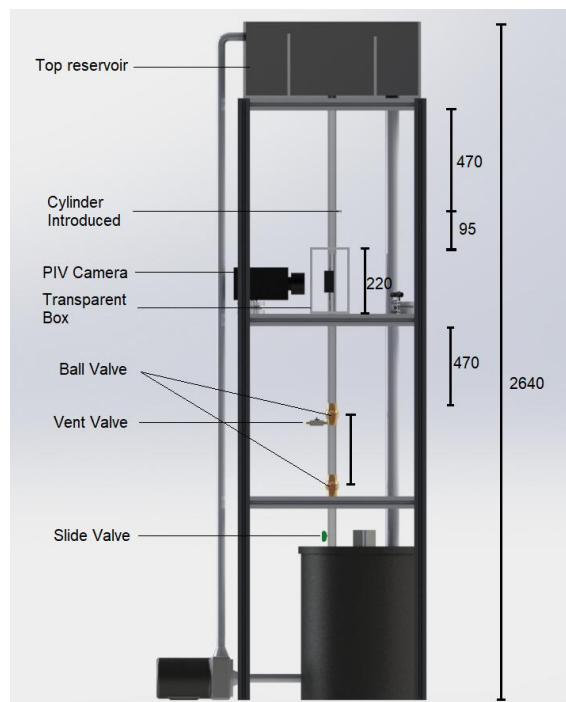


Figure 1. Experimental Set-up. All the dimensions on the image are in millimeter.

3. RESULTS AND DISCUSSION

The first step was to observe how the flow was affected with the insertion of a cylinder. For this reason, measurements with PIV method were made for the flow without the intrusion and afterwards with the cylinder inserted.

Figure 2 shows the comparison between these two cases at a flow rate of $16 \times 10^{-5} \text{ m}^3/\text{s}$.

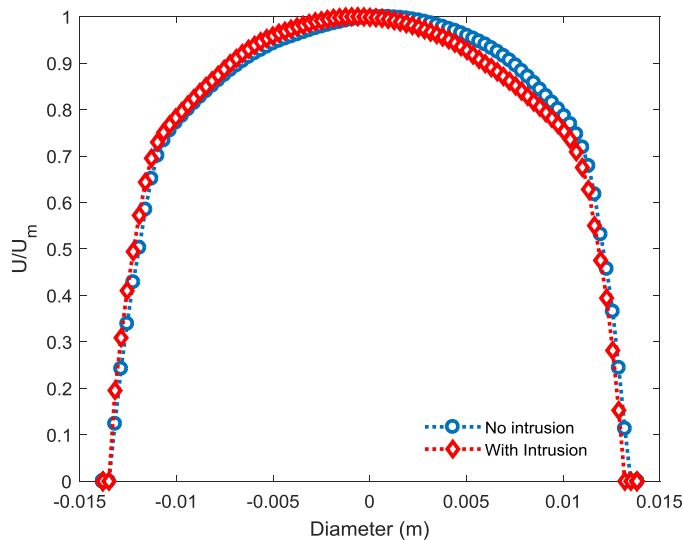


Figure 2. Comparison between the velocity profile with the intrusion and without it for a flow rate of $16 \times 10^{-5} \text{ m}^3/\text{s}$.

It can be seen that the velocity profile is altered on the side of the intrusion. However, the difference between the profiles is small, thus the intrusion was able to fix the bubble position providing reliable experiment results similar to real situations where the Taylor bubble occurs. After understanding the influence of the intrusion on the flow, experiments with the bubble could be conducted.

The experiments with the bubble were performed for different flow rates to show the influence of downward liquid velocity on symmetry and speed of Taylor bubbles. For reference one experiment was performed for a stagnant fluid and the others for downward flow with different flow rates.

It was observed that in stagnant liquid the bubble rises quickly and has an axisymmetric shape. However, according to Fabre et al (2014), a different behavior can be seen for downward flow. In this last case, a strong transition occur at the beginning of the bubble movement. Initially the bubble retreat, changing its shape and afterwards it reaches stability. Afterwards the bubble begins to ascend but no longer with a symmetrical shape.

The results of the velocity fields of the flow that surrounds the bubble can be found bellow. Results depicted in the velocity fields correspond to an average of 200 instantaneous fields.

An example of image obtained before processing can be seen in Fig. 3. This image shows the stagnant fluid case and it is possible to see the symmetric shape.



Figure 3. Rising bubble picture before processing. Stagnant flow case.

It is also possible to see the tracing particles in Fig. 3. Using the PIV method, an average velocity field was obtained enabling better analysis.

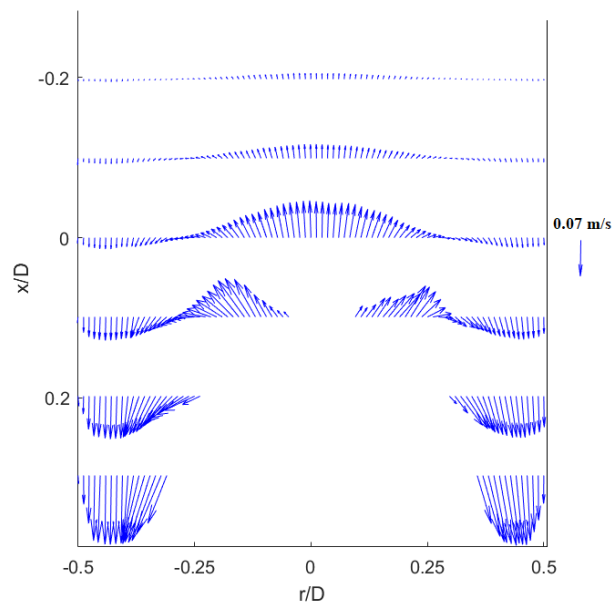


Figure 4. Velocity field surrounding the bubble in stagnant fluid case.

It can be seen in Fig. 4 the flow surrounding the bubble. Far from the nose the velocity is close to zero, as expected. However, the flow closer to the nose is disturbed by the ascendant movement of the bubble, which pushes the flow ahead of it. In the bubble interface, it can be seen an increase of the radial velocity that gradually becomes the flow of the liquid film, this behavior was also observed by Polonsky et al. (1999). The velocity profile of different regions in the image above is shown in Fig. 5.

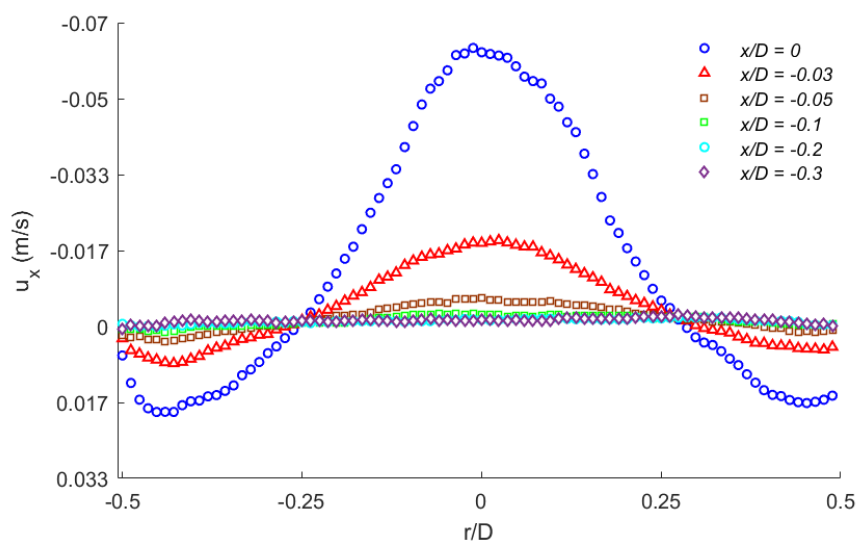


Figure 5. Axial velocity profiles in different regions of the Fig. 4.

It is easier to see in Fig. 5 that the velocity increases where the liquid film is thinner, between the wall and the bubble, satisfying the continuity equation. Closer to the wall the velocity decreases due to friction. The results are in good agreement with the experiment results of Nogueira et al. (2006), where they used a solution of water and glycerol though.

After having a good reference, the flow rate was increased to $5.4 \times 10^{-5} \text{ m}^3/\text{s}$ and the asymmetrical shape could already be seen. An averaged velocity field of the asymmetrical case could be acquired for the first time seen in literature as the bubble is always fixed in the same radial position.

Figure 6 shows the image acquired with the PIV camera before processing.

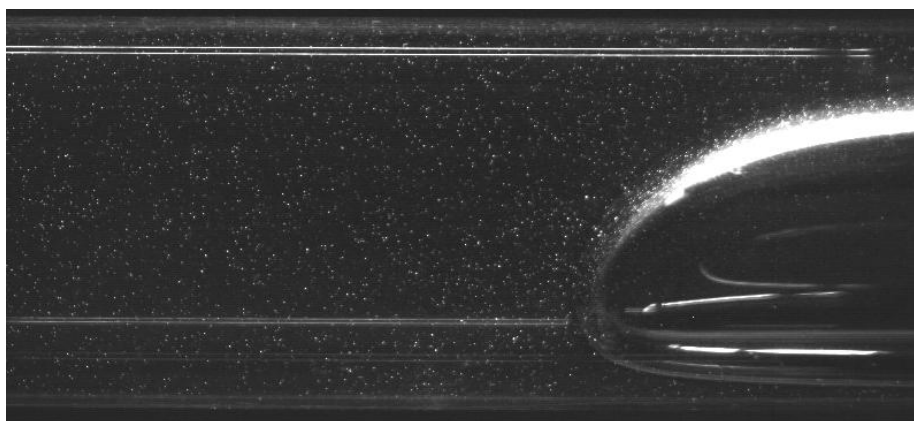


Figure 6. Bubble rising against downward flow, $7.5 \times 10^{-5} \text{ m}^3/\text{s}$.

After removing the mean image in order to remove glass glare and allow better visualization of the particles, the PIV method was used, resulting in Fig. 7. A mask was used to cover the bubble shape and avoid the detection of particles through the bubble by the program. The mask was made using MATLAB.

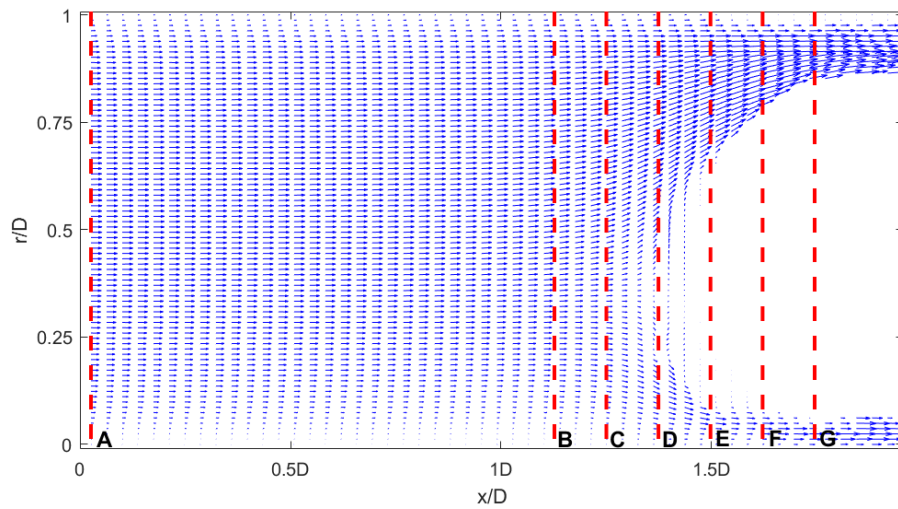


Figure 7. Velocity field surrounding the bubble for flow rate of $7.5 \times 10^{-5} \text{ m}^3/\text{s}$.

Figure 7 shows that the nose of the bubble tends to one side of the wall and it also assumes a more flattened shape. The average velocity field surrounding the bubble nose shows that close to one side of the wall the velocity is almost inexistent. The graphic was divided in seven regions to observe the velocity profile of the liquid flow as it approaches the bubble.

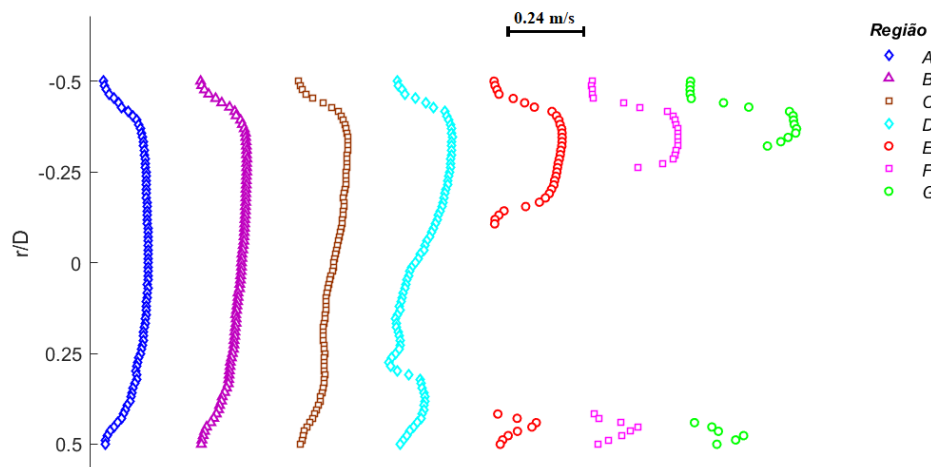


Figure 8. Velocity profile in different regions, flow rate of $7.5 \times 10^{-5} \text{ m}^3/\text{s}$.

Figure 8 shows the velocity profile in each region determined in Fig. 7. The velocity profile of region A is slightly asymmetric due to the intrusion. As the flow approaches the bubble, the flow starts to divide in two different regions, one being bigger than the other due to the asymmetric behavior of the bubble. As in the stagnant case, when the flow passes between the bubble and the wall, the flow speed increases satisfying the continuity equation. The velocities in this case are much higher than the stagnant case.

It can be noticed in Fig. 9 that with the increase of the flow rate the bubble becomes more squished against the pipe wall in order to avoid the higher velocities in the centre of the tube as observed in Fabre and Figueroa-Espinoza (2014).

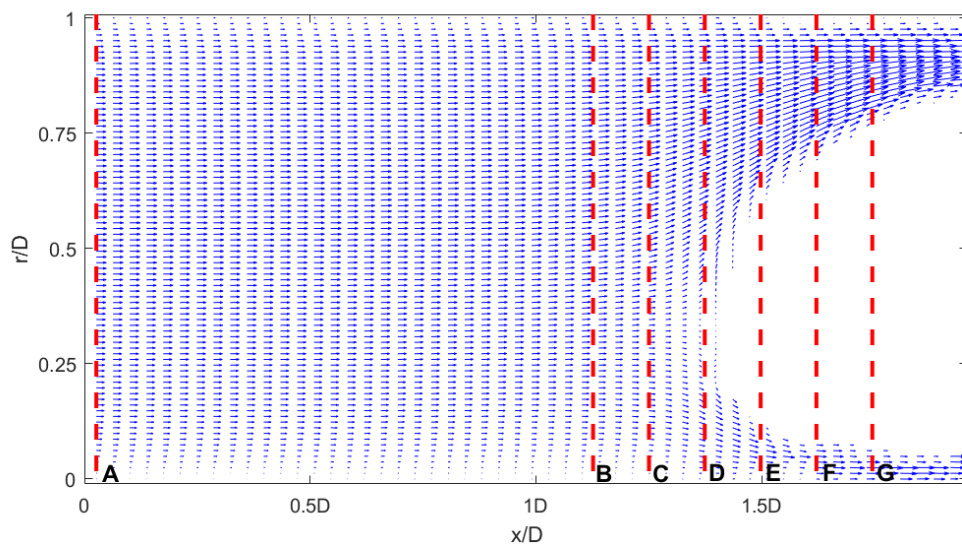


Figure 9. Velocity field surrounding the bubble for flow rate of $9.5 \times 10^{-5} \text{ m}^3/\text{s}$.

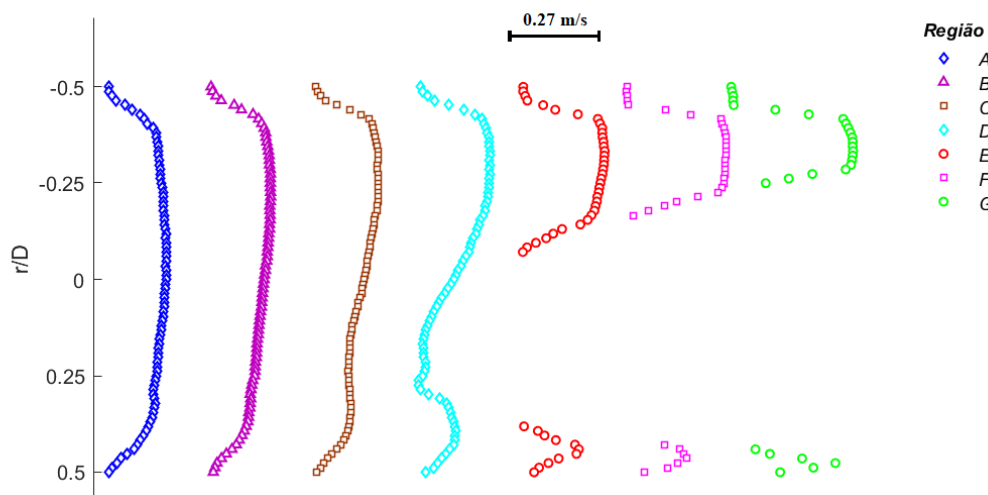


Figure 10. Velocity profile for different regions. Flow rate of $9.5 \times 10^{-5} \text{ m}^3/\text{s}$.

Figure 10 shows that when the flow rate is increased the flow speed between the wall and the bubble also increases. It is possible to see a pattern in the velocity profile before reaching the bubble. As in the other cases, the bubble always tends to fix on the wall where the liquid flow speed is lower, explaining why the intrusion was effective on fixing the radial position.

When the flow rate is increased to $16.5 \times 10^{-5} \text{ m}^3/\text{s}$, the bubble starts to move downwards. As the bubble moves downward, to perform this experiment, first the generated bubble needs to rise above the test section and under the intrusion, only then the desired flow rate is set. shows the averaged velocity field of the flow at $16.5 \times 10^{-5} \text{ m}^3/\text{s}$.

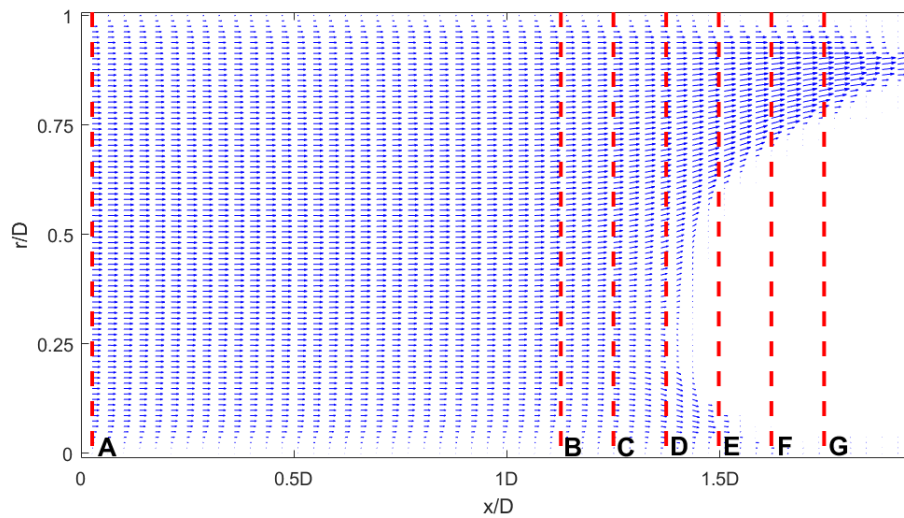


Figure 11. Velocity field surrounding the bubble for flow rate of $16 \times 10^{-5} \text{ m}^3/\text{s}$.

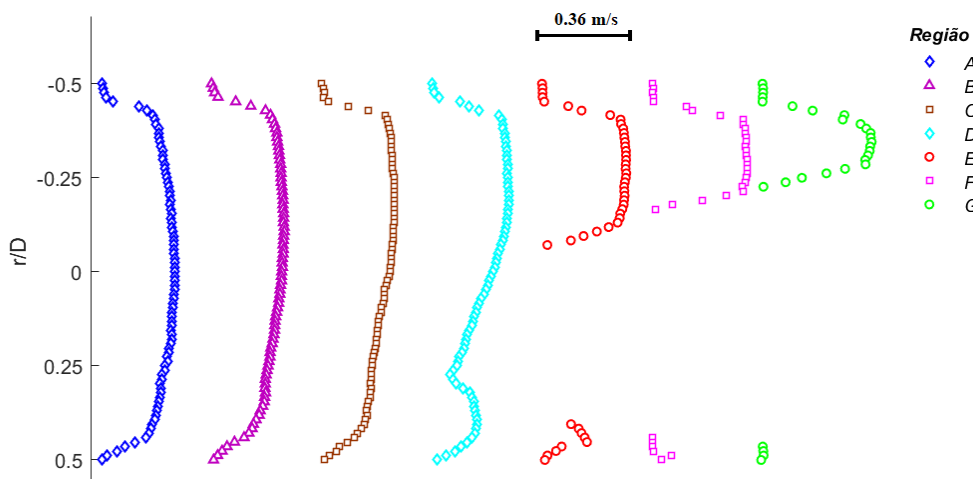


Figure 12. Velocity profile for different regions. Flow rate of $16 \times 10^{-5} \text{ m}^3/\text{s}$.

It is possible to see in Fig. 12 the increase of velocity surrounding the bubble. The shape of is more squished than the previous cases, however the asymmetry seems to become more constant at determined flow rate value. It is difficult to obtain data of the liquid film under the bubble because of the bubble reflections that dazzle the tracing particles.

When the flow rate is increased to $20 \times 10^{-5} \text{ m}^3/\text{s}$, the space between the intrusion and the test section is not big enough to make the change of flow rate without touching the intrusion or without making the bubble instable due to the quick change. For this reason, in this case while rising the bubble before setting the correct flow rate, the bubble was positioned above the intrusion. In this case, the bubble radial position changed to the opposite side, the reason for this behavior is attributed to the attraction of the bubble to the intrusion, making the bubble to stick at the same side of it. The results of this test can be seen in.

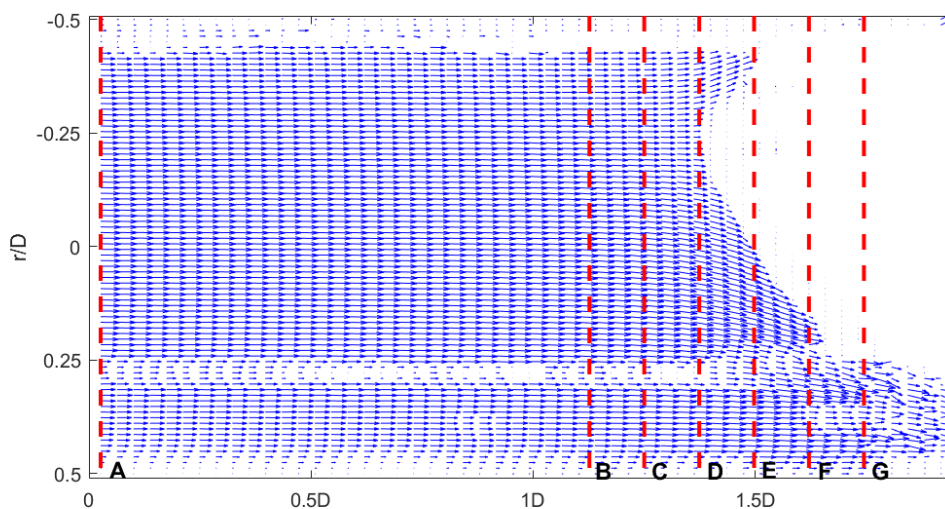


Figure 13. Velocity field surrounding the bubble for flow rate of $20 \times 10^{-5} \text{ m}^3/\text{s}$.

The results obtained in this case were affected by the reflections of the bubble and causes the gaps seen in Fig. 13. These reflections were cut of the velocity profiles in Fig. 14.

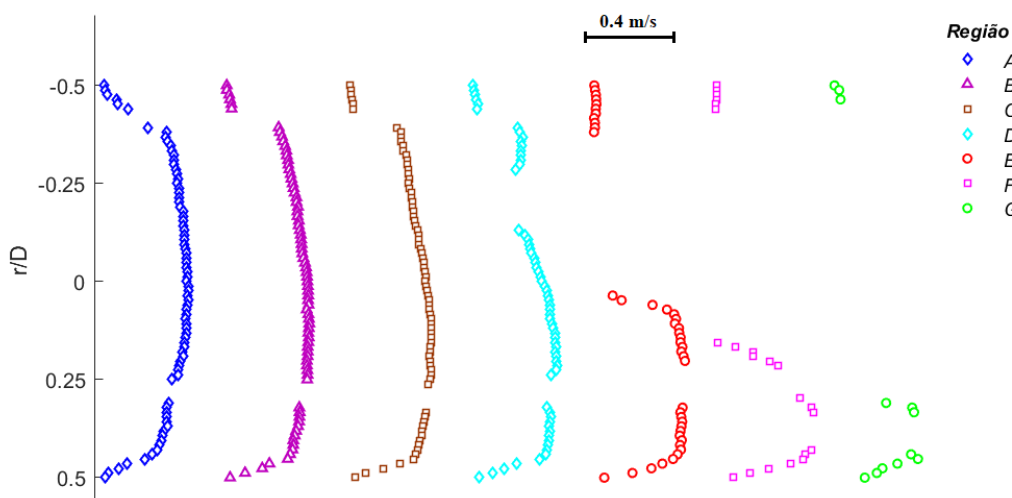


Figure 14. Velocity profile for different regions. Flow rate of $20 \times 10^{-5} \text{ m}^3/\text{s}$.

Figure 14 shows that the velocity profile is slower on the same side that the bubble fixates, demonstrating again the behavior of the bubble trying to escape the high flow speeds.

4. CONCLUSION

Through the insertion of an intrusion in the flow before reaching the bubble, the radial position could be fixed allowing the employment of the PIV method. This intrusive method slightly distorts the flow, providing reliable results similar to the case without the intrusion.

Average velocity fields surrounding the asymmetric bubble were successfully obtained for the first time in literature. The experiment provided information for three different flow rates ($7.5 \times 10^{-5} \text{ m}^3/\text{s}$; $9.5 \times 10^{-5} \text{ m}^3/\text{s}$ and $16 \times 10^{-5} \text{ m}^3/\text{s}$) and for the $20 \times 10^{-5} \text{ m}^3/\text{s}$ case, the reflections of the bubble affected the results.

The velocity field surrounding the bubble in stagnant flow conditions is presented and compared with the work of Nogueira et al. (2006), showing good agreement between the results. It is possible to see the increase of velocity as the

flow passes the thinner space between the bubble and the wall, satisfying the continuity equation. Moreover, the velocity decreases as it approaches the pipe wall as predicted in the theory.

The results presented in this paper show evidence that the bubble avoids the high velocities of the flow as observed in Fabre e Figueroa-Espinoza (2014). The bubble always fix its position where the flow in front of it has lower velocity. These results also indicate that the main factor which determines the bubble positioning is the flow ahead of it (Collins et al. 1978).

It must be noted that the case studied in this work only analyze the Taylor bubble in a 2D plane, for this reason, the shape of the bubble obtained could only be the biggest one. However, the results here obtained serve as an initial advance in the study regarding asymmetric Taylor bubbles in a downward flow.

5. REFERENCES

- Collins, R. et al., 1978. "The motion of a large gas bubble rising through liquid flowing in a tube". *Journal of Fluid Mechanics*.
- Davies, R. M.; Taylor, G, 1950. "The Mechanics of Large Bubbles Rising through Extended Liquids and through Liquids in Tubes". *Proceedings of the Royal Society A: Mathematical, Physical and Engineering Sciences*.
- Dumitrescu, D. T., 1943. "Strömung an einer Luftblase im senkrechten Rohr". *ZAMM - Journal of Applied Mathematics and Mechanics / Zeitschrift für Angewandte Mathematik und Mechanik*.
- Fabre, J.; Figueroa-Espinoza, B., 2014. "Taylor bubble rising in a vertical pipe against laminar or turbulent downward flow: symmetric to asymmetric shape transition". v. 755, p. 485–502.
- Goldsmith, H. L.; Mason, S. G., 1962. "The movement of single large bubbles in closed vertical tubes". *Journal of Fluid Mechanics*.
- Kawaji, M. et al. , 1993. "Flow visualization of two-phase flows using photochromic dye activation method". *Nuclear Engineering and Design*.
- Lu, X.; Prosperetti, A., 2006. "Axial stability of Taylor bubbles". *J. Fluid Mech*, v. 568, p. 173–192.
- Martin, C. S., 1976. "Vertically Downward Two-Phase Slug Flow". *Journal of Fluids Engineering*.
- Nicklin, D. J.; Wilkes, M. A.; Davidson, J. F., 1962. "Two-Phase Flow in Vertical Tubes". *Transactions of the Institution of Chemical Engineers*.
- Nogueira, S. et al. "Flow in the nose region and annular film around a Taylor bubble rising through vertical columns of stagnant and flowing Newtonian liquids". *Chemical Engineering Science*, v. 61, p. 845–857, 2006.
- Polonsky, S.; Shemer, L.; Barnea, D., 1999. "The relation between the Taylor bubble motion and the velocity ahead of it". *International Journal of Multiphase Flow*.
- White, E. T.; Beardmore, R. H., 1962. "The velocity of rise of single cylindrical air bubbles through liquids contained in vertical tubes". *Chemical Engineering Science*.